

See discussions, stats, and author profiles for this publication at: <https://www.researchgate.net/publication/42372613>

Self-poisoning of *Mycobacterium tuberculosis* by targeting GlgE in an α -glucan pathway

Article in *Nature Chemical Biology* · March 2010

Impact Factor: 13 · DOI: 10.1038/nchembio.340 · Source: PubMed

CITATIONS

74

READS

138

10 authors, including:



[Rainer Kalscheuer](#)

Heinrich-Heine-Universität Düsseldorf

49 PUBLICATIONS 2,184 CITATIONS

[SEE PROFILE](#)



[Usha Veeraraghavan](#)

University of Birmingham

25 PUBLICATIONS 343 CITATIONS

[SEE PROFILE](#)



[Stephen Bornemann](#)

John Innes Centre

62 PUBLICATIONS 1,447 CITATIONS

[SEE PROFILE](#)



[William R Jacobs](#)

Howard Hughes Medical Institute

303 PUBLICATIONS 11,011 CITATIONS

[SEE PROFILE](#)

Self-poisoning of *Mycobacterium tuberculosis* by targeting GlgE in an α -glucan pathway

Rainer Kalscheuer^{1,5}, Karl Syson², Usha Veeraraghavan³, Brian Weinrick¹, Karolin E Biermann¹, Zhen Liu⁴, James C Sacchettini⁴, Gurdyal Besra³, Stephen Bornemann² & William R Jacobs Jr^{1*}

New chemotherapeutics are urgently required to control the tuberculosis pandemic. We describe a new pathway from trehalose to α -glucan in *Mycobacterium tuberculosis* comprising four enzymatic steps mediated by TreS, Pep2, GlgE (which has been identified as a maltosyltransferase that uses maltose 1-phosphate) and GlgB. Using traditional and chemical reverse genetics, we show that GlgE inactivation causes rapid death of *M. tuberculosis* *in vitro* and in mice through a self-poisoning accumulation of maltose 1-phosphate. Poisoning elicits pleiotropic phosphosugar-induced stress responses promoted by a self-amplifying feedback loop where trehalose-forming enzymes are upregulated. Moreover, the pathway from trehalose to α -glucan exhibited a synthetic lethal interaction with the glucosyltransferase Rv3032, which is involved in biosynthesis of polymethylated α -glucans, because key enzymes in each pathway could not be simultaneously inactivated. The unique combination of maltose 1-phosphate toxicity and gene essentiality within a synthetic lethal pathway validates GlgE as a distinct potential drug target that exploits new synergistic mechanisms to induce death in *M. tuberculosis*.

M*ycobacterium tuberculosis* (Mtb), the etiological agent of tuberculosis (TB), is the leading cause of mortality due to bacterial pathogens, claiming about 2 million lives annually. With the advent of the antibiotic era, TB became treatable, and at one point eradication was believed possible. However, in recent years TB has reemerged as a major global health threat due to poverty, a deadly synergy with HIV, and the emergence of extensively drug-resistant strains (XDR-TB) that are virtually untreatable with current chemotherapies¹. To counter this resurgence of TB, new treatment options are urgently needed based on new classes of bacterial targets that are very different from those of the antibiotics currently in use.

Identification of essential gene functions required for *in vitro* growth of Mtb is a pivotal strategy for discovering new drug targets owing to the ease of screening for antibacterial compounds. A genome-wide screen of a saturated Mtb transposon mutant library indicated that more than 600 genes (~15%) may be required for *in vitro* growth². However, the rational development of specific inhibitors is hampered by ignorance of the functions of many of these essential candidates. Identification of nonessential gene functions dispensable for *in vitro* growth but required for virulence is an additional valuable source of drug targets. 194 of the nonessential Mtb genes were predicted to be specifically required for *in vivo* growth in mice³. Given that Mtb is an obligate intracellular pathogen highly adapted to the human host, with no known environmental niche, the large number of genes dispensable for *in vitro* growth and virulence is surprising. This high degree of gene dispensability probably reflects extensive genetic redundancy or functional homeostatic buffering within essential processes, so that mutations in single genes are often compensated for by other genes. This means that many 'synthetic lethal' pathways are certainly present in Mtb. 'Synthetic lethality' describes any combination of two separately nonlethal mutations that jointly lead to inviability. Synthetic lethal

genetic interactions have been demonstrated in genome-wide studies of yeast, revealing that most nonessential yeast genes have several synthetic lethal interactions with other genes^{4,5}. Identification of synthetic lethal pathways in Mtb would thus greatly increase the repertoire of drug target candidates.

Here we describe the discovery of a new four-step pathway from trehalose to α -glucan in Mtb comprising the enzymes TreS, Pep2, GlgE and GlgB. The key enzyme in this pathway is the essential maltosyltransferase GlgE, which uses maltose 1-phosphate (M1P) as the donor substrate. Inactivation of either GlgE or GlgB led to self-poisoning by the accumulation of the phosphosugar M1P, driven by a self-amplifying feedback stress response. A combination of traditional and chemical reverse genetics demonstrated the lethal effect of GlgE inactivation for Mtb grown both *in vitro* and in mice. Moreover, we found a synthetic lethal interaction with a pathway leading to polymethylated α -glucans in Mtb. This unique combination of gene essentiality within a synthetic lethal pathway validates GlgE as a new potential Mtb drug target candidate by suggesting possible mechanisms for boosting the potency of inhibitors and for suppressing resistance mutations. To our knowledge, this is the first time α -glucan synthesis has been described as a potential target for antimicrobials.

RESULTS

Validation of the essentiality of *glgE* in Mtb

Analysis of the function of essential genes could define new drug target candidates for the treatment of XDR-TB strains. One such candidate, *glgE* (Rv1327c), has been predicted to be essential for *in vitro* growth of Mtb². The *glgE* homolog was also suggested to be essential in *Mycobacterium smegmatis*⁶. In addition to its presumed essentiality, GlgE fulfills further criteria that suggest it could be an excellent drug target: GlgE homologs are absent from humans and from commensal gut flora bacteria, but are present

¹Howard Hughes Medical Institute, Department of Microbiology and Immunology, Albert Einstein College of Medicine, Bronx, New York, USA.

²Department of Biological Chemistry, John Innes Centre, Norwich Research Park, Norwich, UK. ³School of Biosciences, University of Birmingham, Edgbaston, Birmingham, UK. ⁴Texas A&M University, Department of Biochemistry and Biophysics, College Station, Texas, USA. ⁵Present address: Institute for Medical Microbiology and Hospital Hygiene, Heinrich-Heine-University Düsseldorf, Düsseldorf, Germany. *e-mail: jacobs@hhmi.org

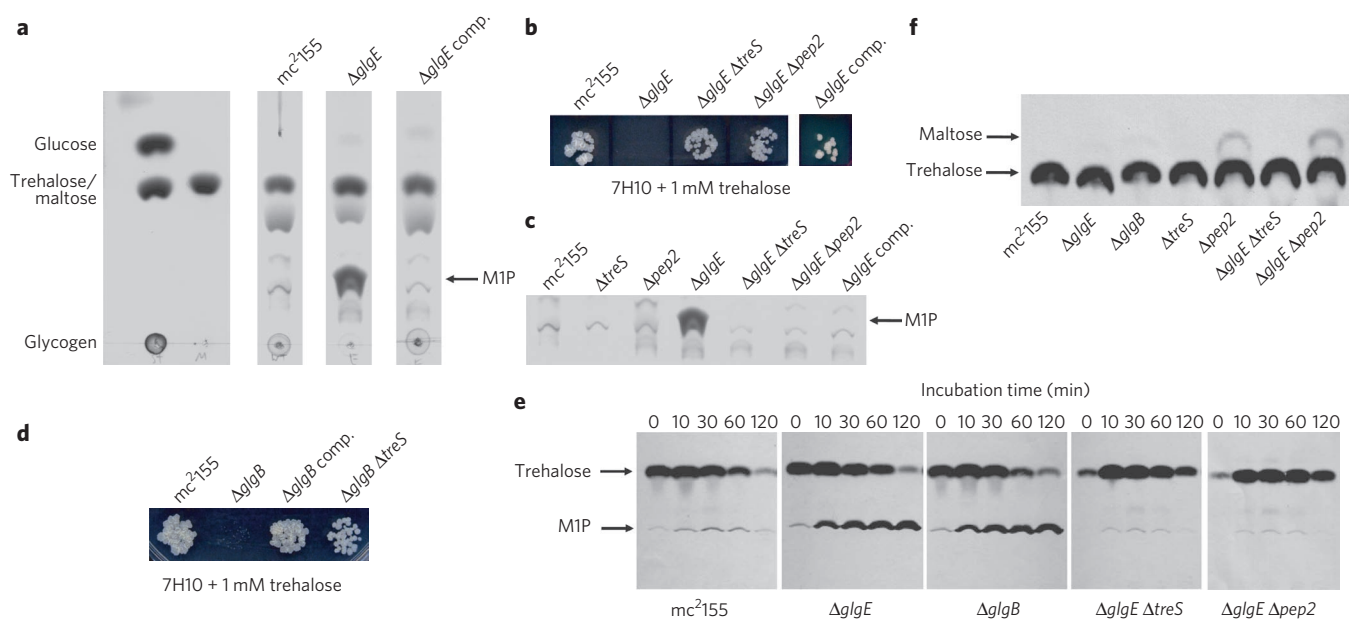


Figure 1 | Characterization of the *M. smegmatis* Δ *glgE* mutant. (a) M1P accumulation in the Δ *glgE* mutant, as revealed by TLC analysis of cell extracts from 48-h-old cultures. See **Supplementary Figure 9** for a full, uncut TLC image. (b) Trehalose sensitivity of the Δ *glgE* mutant. (c) Abolition of M1P accumulation by suppressor mutations in the Δ *glgE* mutant, as revealed by TLC analysis of cell extracts from 48-h-old cultures. (d) Trehalose sensitivity of the Δ *glgB* mutant. (e) M1P accumulation in the Δ *glgE* and Δ *glgB* mutants determined by TLC/autoradiography analysis of extracts from cells labeled with ¹⁴C-trehalose for the indicated time intervals. (f) Maltose accumulation in Δ *pep2* mutant strains determined by TLC/autoradiography analysis of cell extracts from cells labeled with ¹⁴C-trehalose for 30 min. In **b** and **d**, equal dilutions of cultures were spotted onto Middlebrook 7H10 agar plates containing trehalose. 'Comp.' refers to mutants complemented with the respective WT genes.

in almost all mycobacteria and in some opportunistic pathogens, such as *Pseudomonas* and *Burkholderia* species.

To verify the essentiality of *glgE* in *Mtb*, we compared the frequencies of generating *glgE* deletion mutations in the wild type (WT) to those in an isogenic merodiploid strain containing a second copy of *glgE* provided on an integrative single-copy plasmid, using specialized transduction. Transductants with a deleted WT allele were obtained only in the merodiploid strain, at a frequency of 4.08×10^{-9} . We were unable to obtain transductants in the haploid strain despite repeated attempts (frequency $< 6 \times 10^{-11}$), thus confirming *glgE* essentiality in *Mtb* (see **Supplementary Fig. 1a,b** in **Supplementary Results**).

Accumulation of M1P in *M. smegmatis* Δ *glgE*

Because *glgE* is clustered with genes coding for enzymes with known involvement in glycogen metabolism, such as the branching enzyme GlgB and the glycogen phosphorylase GlgP (**Supplementary Fig. 1a**), and because GlgE resembles α -amylases, GlgE has been proposed to be involved in glycogen degradation. The demonstration that thermal inactivation of GlgE in a temperature-sensitive *M. smegmatis* mutant strain apparently leads to increased glycogen accumulation and unexpected cell toxicity was interpreted as supporting the hypothesis that GlgE was a mediator of glycogen degradation⁶. However, because high glycogen levels are not usually found to be toxic to bacteria, and because many bacteria capable of synthesizing and remobilizing glycogen lack a *glgE* ortholog, we sought an alternative explanation for the gene essentiality.

To reexamine GlgE function, we attempted deletion of the *glgE* homolog in *M. smegmatis*. In contrast to GlgE's suggested essentiality⁶, null deletion mutations could be readily generated on a minimal medium, allowing inferences on GlgE function from phenotypical mutant characterization. TLC analysis of hot water extracts from the *M. smegmatis* Δ *glgE* mutant revealed no increased glycogen content, but we did observe large amounts of a low-molecular-weight carbohydrate (**Fig. 1a**). This substance was purified by size exclusion

chromatography followed by preparative TLC, and subjected to various chemical analyses (**Supplementary Fig. 2**) that identified the substance as α -D-glucopyranosyl(1 \rightarrow 4)- α -D-glucopyranosyl 1-phosphate (maltose 1-phosphate, M1P). To quantify glycogen in the temperature-sensitive *glgE* mutant, a coupled enzymatic reaction was used that measures glucose released upon amyloglucosidase treatment of extracted polysaccharides⁶. Because amyloglucosidase has no molecular weight specificity, the coupled assay would not have discriminated between M1P and glycogen, leading to a likely misinterpretation.

A functional link between GlgE, GlgB, TreS and Pep2

Surprisingly, despite normal growth in minimal medium (Middlebrook 7H9), the *M. smegmatis* Δ *glgE* mutant could not grow in complex media (for example, LB medium). To identify the growth-inhibitory components in LB medium, we tested the sensitivity of the *M. smegmatis* Δ *glgE* mutant toward various mono- and disaccharides and found that it was sensitive to the disaccharide trehalose (α -D-glucopyranosyl-(1 \rightarrow 1)- α -D-glucopyranoside). This is surprising given that this sugar is abundant in mycobacteria, and yet a concentration of 0.5 mM completely inhibited growth of the mutant (**Fig. 1b**). Trehalose induced bacteriostasis in *M. smegmatis* Δ *glgE* correlating with M1P hyperaccumulation (**Supplementary Fig. 3**).

Spontaneous mutations restoring growth of *M. smegmatis* Δ *glgE* in the presence of trehalose were observed at a frequency of 4.5×10^{-5} . In order to identify the presumed suppressor mutations abolishing trehalose sensitivity, a transposon mutant library of *M. smegmatis* Δ *glgE* was screened by selecting for resistance to 1 mM trehalose. Mapping of the transposon insertion sites in trehalose-insensitive Δ *glgE* mutants identified the trehalose synthase gene *treS* (encoding a Rv0126 homolog) as a target in several independent clones. To confirm the transposon mutant phenotypes, we deleted *treS* in an unmarked *M. smegmatis* Δ *glgE* strain by specialized transduction. Additionally, we separately deleted *pep2* (encoding a Rv0127 homolog), which is clustered with *treS* in many bacteria. Both

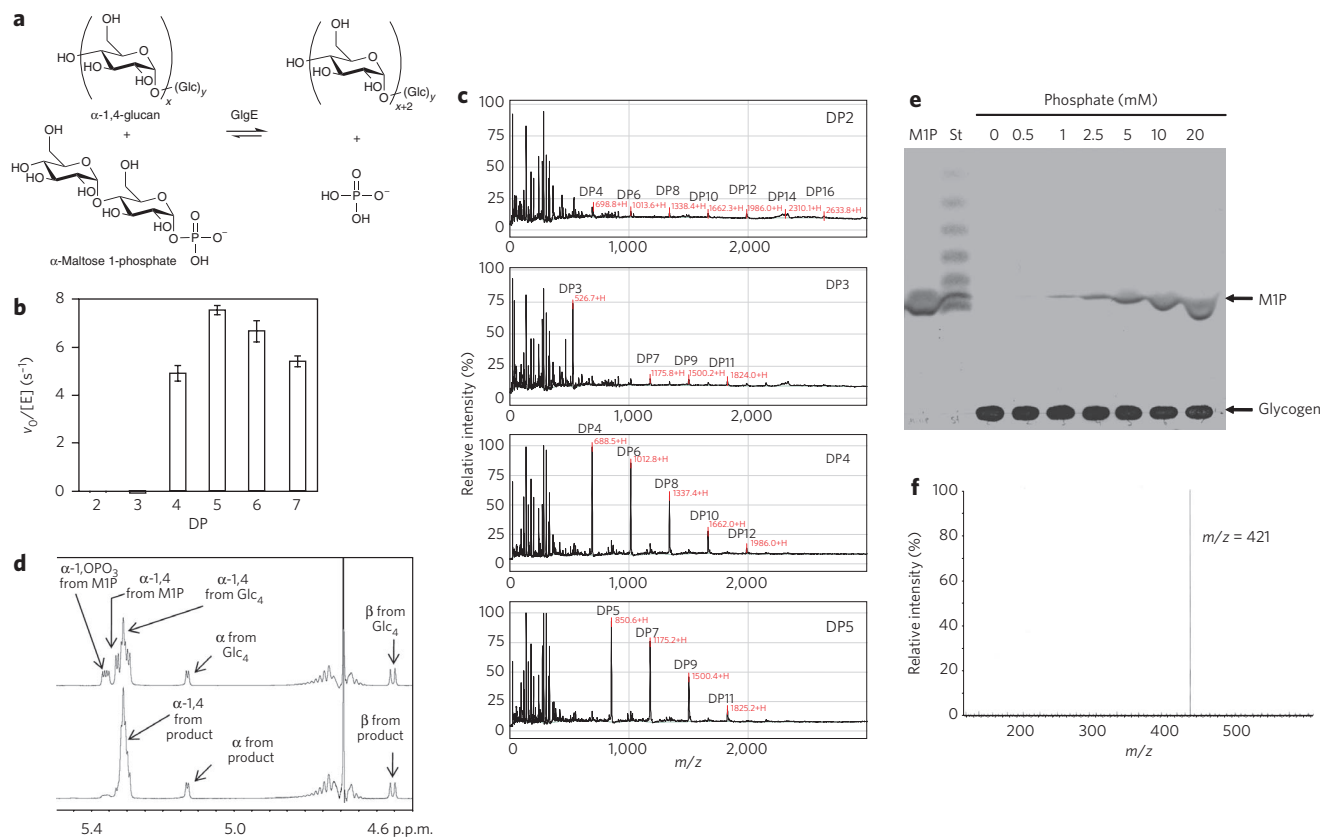


Figure 2 | GlgE is a new M1P-dependent maltosyltransferase. (a) Proposed reaction catalyzed by GlgE. x and y indicate number of glucose units. (b) Acceptor specificity of Mtb GlgE. Enzyme activity with maltooligosaccharide acceptor substrates was determined by monitoring phosphate release in triplicate. The bars indicate means \pm s.e.m. (c) Mass spectra showing the extension of maltooligosaccharides (DP2 after 22 h; DP3, DP4 and DP5 after 1 h) by GlgE in the presence of M1P. Maltooligosaccharides were detected as $[M+Na]^+$ ions. (d) Determination of the glycosidic linkage formed by GlgE monitored using 1H NMR spectroscopy. The upper spectrum shows a control without enzyme, and the lower spectrum shows the reaction with enzyme after completion according to the phosphate release assay. Peak assignments are as indicated. (e) Release of M1P from glycogen by Mtb GlgE in the presence of inorganic phosphate analyzed by TLC. St, maltooligosaccharide standards (glucose through maltoheptaose). (f) ESI-MS analysis of M1P formed in e with an expected mass for $[M-H]^-$ of 421 Da. Accurate mass spectrometry in positive mode gave a mass of 467.05304 with an expected mass of 467.05371 for $[M+Na_2+H]^+$, giving an error of <2 p.p.m.

second-site gene deletions conferred trehalose resistance and suppressed M1P accumulation caused by *glgE* inactivation (Fig. 1b,c).

The *glgB* gene (Rv1326c) clusters with *glgE* and encodes a branching enzyme that is required for introducing α -1,6-linked branches into linear α -1,4-glucans⁷, which was demonstrated to be essential in Mtb H37Rv (ref. 8). As for *glgE*, however, we found *glgB* to be nonessential in *M. smegmatis*. Moreover, the *M. smegmatis* Δ *glgB* mutant was also sensitive to trehalose. Trehalose sensitivity in an unmarked *M. smegmatis* Δ *glgB* strain could again be suppressed by deletion of *treS* (Fig. 1d).

Trehalose synthase (TreS) mediates the reversible interconversion of trehalose and maltose^{9,10}. Pep2 from Mtb has not been characterized but is homologous to the maltokinase Mak1 from phylogenetically related actinomycetes (*Actinoplanes missouriensis* and *Streptomyces coelicolor*) that phosphorylates maltose to M1P using ATP¹¹. The clustering of *treS* and *pep2* thus suggests that M1P is synthesized from trehalose via maltose by sequential reactions mediated by TreS and Pep2. To corroborate this, *M. smegmatis* mutant strains were labeled with ^{14}C -trehalose (Fig. 1e). Radiolabeled trehalose was rapidly taken up and metabolized to M1P in the Δ *glgE* mutant. Also, *glgB* deletion led to a rapid accumulation of M1P, whereas this phosphosugar never reached high levels in the WT. Inactivation of *treS* or *pep2* prevented M1P formation in the Δ *glgE* mutant. Substantial levels of the radiolabeled maltose intermediate were detectable only in Δ *pep2* strains, indicating its usual fast turnover to M1P by Pep2

(Fig. 1f). Together, these findings establish a functional link among TreS, Pep2, GlgE and GlgB in *M. smegmatis*. This is supported by the fact that the structural genes, while arranged in two separate chromosomal gene clusters in mycobacteria, often lie in a single locus in many other prokaryotes (Supplementary Fig. 4).

GlgE is a new maltosyltransferase that uses M1P

Cytoplasmic M1P accumulation in the *M. smegmatis* Δ *glgE* mutant suggested that this phosphosugar might be the direct substrate of GlgE. Given that the branching enzyme GlgB uses linear α -1,4-glucan as a substrate⁷, we hypothesized that GlgE could act upstream of GlgB producing such linear glucans. This could be accomplished by transferring the maltosyl moiety of M1P to the nonreducing end 4-OH of an α -glucan acceptor substrate with release of phosphate (Fig. 2a). *In vitro* enzymatic activity of histidine-tagged recombinant GlgE (Supplementary Fig. 5a) was assayed either quantitatively by monitoring phosphate release from M1P, or qualitatively using mass spectrometry or TLC. Maltooligosaccharides with a degree of polymerization (DP) ≥ 4 were efficient acceptors, with DP5 being optimal in the GlgE-catalyzed polymerization of M1P (Fig. 2b,c). The β -anomer of M1P at a 1 mM concentration gave no activity with 1 mM maltohexaose as the acceptor (detection limit was $\leq 1\%$ of the activity with the α -anomer). The presence of α -1,4 links in the oligosaccharide products from maltotetraose extension was shown by NMR spectroscopy (Fig. 2d), with no evidence for other

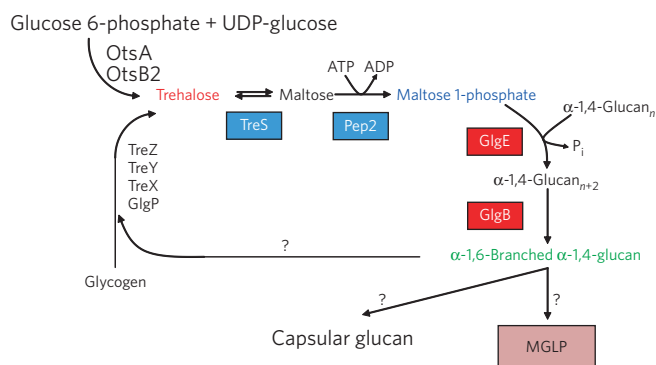


Figure 3 | A new prokaryotic pathway from trehalose to α -glucan.

The reactions involved in conversion of trehalose to α -glucan comprise two essential steps in *Mtb*, catalyzed by GlgE and GlgB. n = number of glucose units.

α -1, n or β -1, n links¹². Together, these observations showed that the enzyme exhibits an α -retaining catalytic mechanism. The activity with maltohexaose was optimal at pH 7.0 and 37 °C, consistent with the lifestyle of the organism (Supplementary Fig. 5b–d).

The K_m^{app} for maltohexaose with 5 mM M1P was 35 ± 8 mM, with a $k_{\text{cat}}^{\text{app}}$ of 15.4 ± 1.1 s⁻¹, revealing a $k_{\text{cat}}^{\text{app}}/K_m^{\text{app}}$ of 440 ± 100 M⁻¹ s⁻¹ (Supplementary Fig. 5e–g), which demonstrates a catalytic efficiency within the typical range for a carbohydrate active enzyme. With 1 mM M1P, the K_m^{app} and $k_{\text{cat}}^{\text{app}}$ of maltohexaose decreased to 13.3 ± 2.4 mM and 7.5 ± 0.4 s⁻¹, respectively, giving a $k_{\text{cat}}^{\text{app}}/K_m^{\text{app}}$ of 570 ± 110 M⁻¹ s⁻¹. This trend, coupled with statistically indistinguishable

values of $k_{\text{cat}}^{\text{app}}/K_m^{\text{app}}$, is consistent with a substituted-enzyme kinetic mechanism (also known as ping pong), whereby the phosphate- and acceptor-binding sites are synonymous, precluding donor and acceptor molecules from binding simultaneously to the enzyme. The K_m^{app} for M1P with 1 mM maltohexaose was 0.25 ± 0.05 mM, with a $k_{\text{cat}}^{\text{app}}$ of 1.26 ± 0.07 s⁻¹, giving a $k_{\text{cat}}^{\text{app}}/K_m^{\text{app}}$ of $5,000 \pm 1,000$ M⁻¹ s⁻¹, which shows that M1P is an efficient donor.

We also tested the reversibility of GlgE activity. Using glycogen as a donor substrate, we found that higher phosphate concentrations resulted in higher M1P production (Fig. 2e,f), confirming reversibility *in vitro*. Using the phosphate assay with 125 mM maltohexaose and 20 mM inorganic phosphate, we found that ~10% of the phosphate was converted to M1P, showing that the equilibrium is in favor of M1P consumption, as would be expected for this activated sugar. The K_m^{app} for inorganic phosphate was estimated to be 6 ± 4 mM (Supplementary Fig. 5h). The enzyme also catalyzed the disproportionation of maltooligosaccharides. Mass spectrometry showed that transfer of maltosyl units from donors with a DP ≥ 4 occurred, but a DP ≥ 6 gave the most rapid transfers (Supplementary Fig. 6a–e). The smallest product of disproportionation had a DP of 4, and the smallest acceptor in this reaction also had a DP of 4 (Supplementary Fig. 6f–i), as was the case with M1P as the donor (Fig. 2b).

The unveiling of the M1P-dependent maltosyltransferase activity of GlgE, in combination with the phenotypes of the *M. smegmatis* mutants, allows the plausible conclusion that GlgE is part of a new pathway in *Mtb* (and many other phylogenetically distant prokaryotes) that converts trehalose into an α -1,6-branched α -1,4-glucan via four enzymatic steps mediated by TreS, Pep2, GlgE and GlgB (Fig. 3 and Supplementary Fig. 4). GlgE not only forms the linear α -1,4-glucan but it can also edit the branch lengths of branched glucan

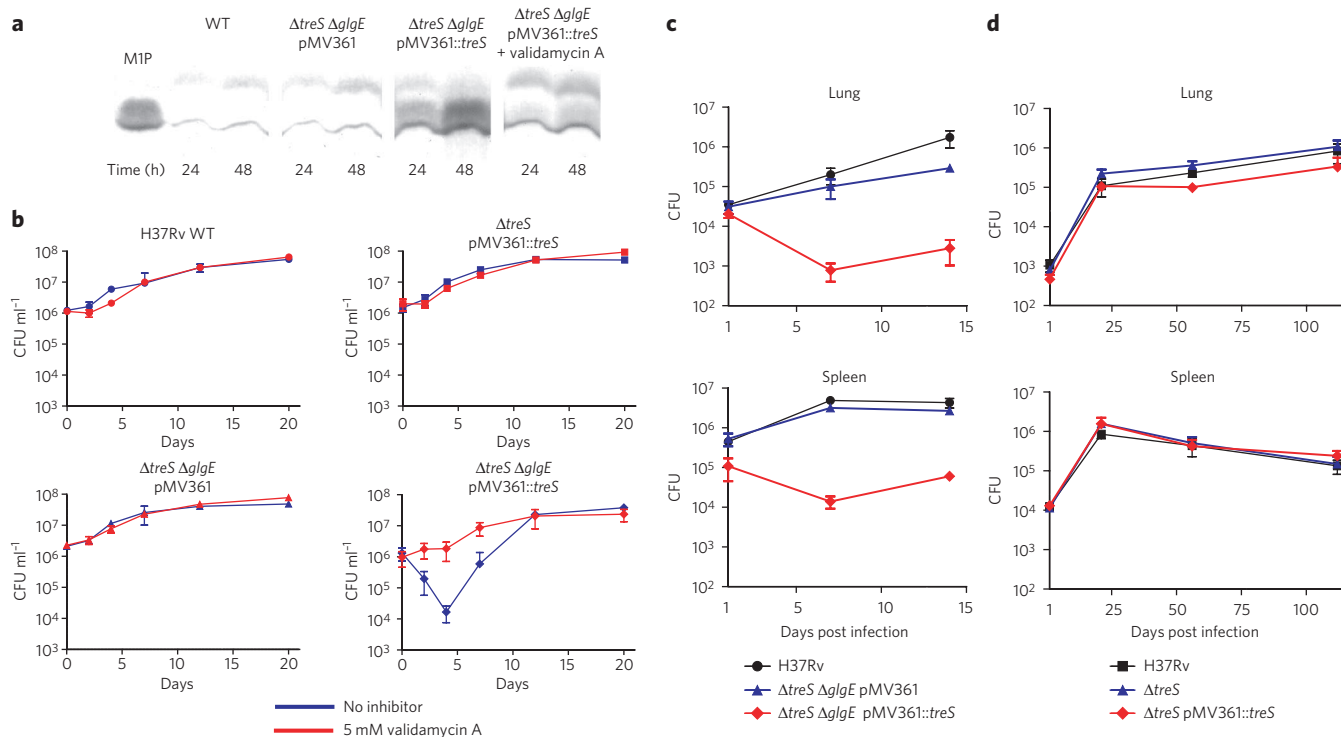


Figure 4 | M1P self-poisoning is lethal for *Mtb* grown *in vitro* and in mice. All strains were precultivated in the presence of 5 mM validamycin A to log phase and then subjected to the indicated conditions. (a) GlgE inactivation causes M1P accumulation in a recombinant *Mtb* H37Rv mutant strain. M1P accumulation was determined by TLC analysis of extracts from cells depleted in validamycin A for 24 or 48 h. See Supplementary Figure 9 for a full, uncut TLC image. (b) GlgE inactivation is bactericidal *in vitro* in liquid culture. Viability was determined by quantifying colony-forming units (CFU). (c) The conditional lethal mutant strain $\Delta treS \Delta glgE$ (pMV361::treS) is killed in a mouse infection model. BALB/c mice were infected intravenously with 10^6 CFU per animal. (d) TreS is dispensable for virulence in mice. BALB/c mice were infected intravenously with 5×10^4 CFU per animal. Bacterial burden in organ homogenates in c and d was determined by counting CFU. The data in b, c and d represent means of triplicates \pm s.d.

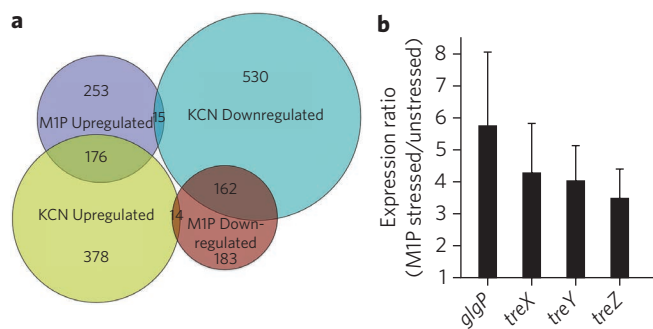


Figure 5 | Whole-genome transcriptional profiling of the M1P-induced stress response in Mtb.

The conditional lethal Mtb mutant strain $\Delta treS \Delta glgE$ (pMV361::treS) and the vector control strain were grown to log phase in the presence of 5 mM validamycin A to suppress M1P formation. Subsequently, cells were washed to remove the inhibitor, and microarrays were performed on cells after 48 h of depletion of validamycin A.

(a) Diagram showing the overlap of the M1P stress response with potassium cyanide (KCN) treatment. Microarray data for KCN treatment have been reported previously¹⁸ and were obtained through the US National Center for Biotechnology Information Gene Expression Omnibus (GEO dataset GSM28256). Only genes with a differential regulation ≥ 2 are included.

(b) Induction of the GlgP-TreX-TreY-TreZ trehalose biosynthetic pathway in M1P-stressed Mtb. Gene expression level was analyzed by qRT-PCR and normalized to 16S rRNA. Expression ratio reported as mean of triplicates \pm s.e.m. See also **Supplementary Figure 7** for the intersections of the M1P stress response with functionally clustered groups of genes (DNA damage response, electron transport chain and ATP synthase, DosR regulon and the translational apparatus) and **Supplementary Figure 8** for qRT-PCR data of other selected transcripts.

with its disproportionation activity. Though three of the four enzymatic activities are well known and have been characterized in Mtb (TreS, GlgB) or related actinomycetes (Pep2), their functional cooperation within a single pathway has eluded precise description due to the lack of awareness of GlgE's key role.

Suppression of *glgE* essentiality by blocking M1P formation

A mutational block in sugar catabolic pathways can cause accumulation of apparently toxic phosphorylated intermediates that render such mutants sensitive to those sugars (for example, refs. 13–15). Similarly, our results with the model organism *M. smegmatis* indicated that M1P accumulation was directly or indirectly toxic, causing the lethality of *glgE* mutations in Mtb. To prove this, we used specialized transduction to compare the frequencies of generating *glgE* deletion mutations in the WT to those in an isogenic unmarked $\Delta treS$ mutant in Mtb, in which M1P formation is blocked. Though we were unsuccessful in deleting *glgE* in the WT, the gene could readily be inactivated in the $\Delta treS$ mutant, confirming both the essentiality of GlgE and the causality of M1P toxicity, respectively (**Supplementary Fig. 1c**). Likewise, *treS* inactivation allowed deletion of *glgB*, demonstrating that M1P toxicity is also the probable cause of GlgB essentiality (**Supplementary Fig. 1d**).

Bactericidal effect of GlgE inactivation in Mtb

Next, we wanted to determine whether inactivation of GlgE causes bacteriostasis or lethality in Mtb. Initial attempts to downregulate the chromosomal expression of *glgE* with a tetracycline-inducible promoter were unsuccessful. In an alternative chemical genetic approach, we tried to generate a *glgE* deletion mutant under conditions in which chemical inhibition of TreS was applied in order to prevent M1P toxicity using the inhibitor validamycin A, which has been demonstrated to inhibit TreS from *Bradyrhizobium* species¹⁶. An approach to delete *glgE* in WT Mtb using specialized transduction

in the presence of validamycin A was unsuccessful. We therefore mimicked the phenotype of a $\Delta glgE$ mutant by complementing the $\Delta treS \Delta glgE$ double mutant of Mtb with a functional copy of the *treS* gene provided on an integrative single-copy plasmid in the presence of validamycin A. As expected, *treS* transformants were obtained in the $\Delta treS \Delta glgE$ mutant only in the presence of validamycin A. We predicted that depletion of the inhibitor would restore TreS enzymatic activity and result in M1P accumulation and cessation of growth in the $\Delta glgE$ surrogate strain. M1P was undetectable by TLC in both the WT Mtb and the vector control strain, and accumulated to only low levels in the $\Delta treS \Delta glgE$ mutant strain carrying pMV361::treS in the presence of 5 mM validamycin A. In contrast, depletion of the inhibitor resulted in copious accumulation of M1P within 48 h in this $\Delta glgE$ surrogate strain (**Fig. 4a**). Importantly, and in contrast to the bacteriostatic effect in *M. smegmatis*, M1P accumulation correlated with rapid killing of the cells *in vitro* in liquid culture (2 log reduction in viability within 4 d) (**Fig. 4b**), demonstrating that GlgE inactivation is lethal in Mtb. Bacteria emerging after the initial killing phase after day 4 did not require supplementation with validamycin A, indicating that they had likely acquired loss-of-function mutations either in the plasmid-encoded *treS* gene or in the chromosomally located *pep2* gene, thus preventing M1P toxicity.

Next, we tested the conditional lethal mutant strain $\Delta treS \Delta glgE$ (pMV361::treS) in a mouse infection model (**Fig. 4c**). This $\Delta glgE$ surrogate strain died rapidly in the lungs and spleens of infected BALB/c mice (about 1.5 log and 1 log reduction of bacterial organ burden within 7 d, respectively). The *in vivo* killing demonstrates that the TreS-Pep2-GlgE-GlgB pathway (henceforth referred to as the GlgE pathway) is active during growth in the host and that endogenous trehalose levels in Mtb are sufficient to support intracellular M1P accumulation reaching lethal concentrations *in vivo*. Bacteria surviving the initial killing phase recovered from spleens and lungs at day 14 were all independent of validamycin A. This again suggests a likely acquisition of loss-of-function mutations in either *treS* or *pep2*, consistent with the absolute necessity of preventing M1P poisoning in order to allow survival *in vivo*.

Together, the *in vitro* and *in vivo* killing phenotypes convincingly validate GlgE's potential as a drug target candidate. It is noteworthy that the kinetics of killing and of emergence of mutants observed with the $\Delta glgE$ surrogate strain *in vitro* resemble those reported for treatment of Mtb with a high concentration of the first-line drug isoniazid¹⁷. Notably, the GlgE pathway as a whole is dispensable for virulence, as demonstrated by the lack of attenuation of the $\Delta treS$ mutant in mice (**Fig. 4d**).

M1P accumulation elicits pleiotropic stress responses in Mtb

In order to gain insight into the molecular mechanisms underlying M1P toxicity and eventual death of Mtb, we performed global gene expression analyses. For this, the conditional lethal Mtb mutant strain $\Delta treS \Delta glgE$ (pMV361::treS) and the vector control strain were grown to log phase in presence of 5 mM validamycin A to suppress M1P formation. Subsequently, cells were washed to remove the inhibitor, and microarrays were performed on cells after 48 h of depletion of validamycin A. We found typical gene expression signatures indicative of unexpected overlapping stress responses in M1P-poisoned Mtb (**Supplementary Fig. 7**; see also **Supplementary Fig. 8** for qRT-PCR confirmation of selected transcripts). A remodeling of the respiratory electron transport chain was obvious, as indicated by significant downregulation of cytochrome *c* oxidase components (encoded by *ctaB*, *ctaC*, *ctaD* and *ctaE*) and upregulation of components of the NADH dehydrogenase I complex (encoded by *nuoB*, *nuoD*, *nuoE* and *nuoF*), of the non-proton-pumping terminal cytochrome *bd* oxidase (encoded by *cydA*, *cydB*, *cydC* and *cydD*) and of nitrate reductase (encoded by *narG*, *narH*, *narI* and *narJ*) (**Supplementary Fig. 7**). Except for

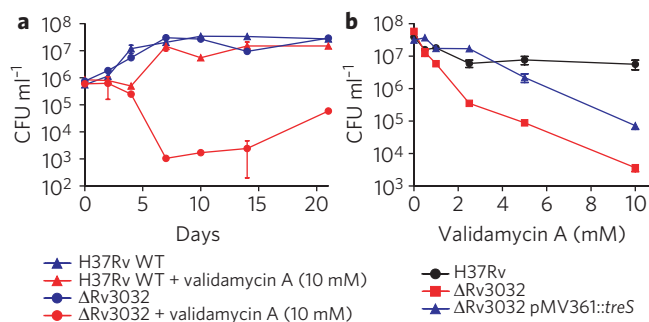


Figure 6 | Synthetic lethality of *treS* and Rv3032. (a) Hypersensitivity of the Mtb Δ Rv3032 mutant toward the TreS inhibitor validamycin A. (b) Low-level resistance of the Mtb Δ Rv3032 mutant against validamycin A mediated by overexpression of the target TreS from an integrative single-copy plasmid. Cultures were inoculated at 5×10^6 CFU ml⁻¹ and cultivated for 7 d. The data in a and b represent means of triplicates \pm s.e.m. Viability was determined by quantifying CFU.

upregulation of NADH dehydrogenase I, this rearrangement resembles known responses to respiratory inhibitors^{18,19}. In fact, in addition to components of the respiratory chain, we observed an overall similarity to the transcription profile elicited by the cytochrome *c* oxidase-specific inhibitor potassium cyanide (Fig. 5a), clearly suggesting that M1P stress unexpectedly results in inhibition of respiration. We also noticed a global downregulation of the dormancy (*dosR*) regulon (Supplementary Figs. 7 and 8). Though the factors triggering induction of this regulon (such as hypoxia, NO and CO) are well characterized^{20,21}, it is unclear which metabolic perturbations stimulate downregulation. Furthermore, expression of most components of ATP synthase (encoded by *atpA*, *atpC*, *atpD*, *atpE*, *atpG* and *atpH*) was significantly downregulated (Supplementary Fig. 7), probably resulting in decreased intracellular ATP levels. This can be linked to the induction of *relA* (Supplementary Fig. 8), which triggers the stringent response²², thus explaining the observed global downregulation of the translational apparatus (Supplementary Fig. 7). Moreover, M1P stress also led to strong induction of the DNA damage-responsive SOS regulon (Supplementary Figs. 7 and 8), including numerous genes involved in DNA repair, such as *recA* and *dnaE2*, which encodes the error-prone DNA polymerase (refs. 18,23). Thus, DNA damage appears to be a surprising direct or indirect outcome of M1P self-poisoning.

Most notably, another distinct stress response was the upregulation of a pathway leading to release of trehalose from glycogen, comprising the genes *glgP*, *treX*, *treY* and *treZ* (Figs. 3 and 5b; Supplementary Fig. 8b)²⁴. Apparently, Mtb reacts to M1P stress by increasing the intracellular trehalose level, perhaps as a stress protectant, given that trehalose has this function in many bacteria and yeasts²⁵. However, in the conditional lethal mutant strain Δ *treS* Δ *glgE* (pMV361::*treS*), this is fatally counterproductive because it promotes further conversion of trehalose to M1P, resulting in a deadly self-amplifying feedback loop that causes progressive self-poisoning.

Synthetic lethality of the GlgE pathway and Rv3032

The new GlgE pathway is not the only biosynthetic route to α -1,4-glucans in Mtb; two alternative pathways have been described⁸. ADP-glucose, formed from glucose 1-phosphate and ATP by the ADP-glucose pyrophosphorylase GlgC, is polymerized by the glycogen synthase GlgA to linear α -1,4-glucans. Alternatively, the glucosyltransferase Rv3032 uses either UDP-glucose or ADP-glucose as the substrate for polymerization to linear α -1,4-glucans⁸. When trying to analyze α -1,4-glucan formation in Mtb by combinatorial inactivation of the three known pathways by targeting key

steps (GlgC, Rv3032, TreS), we found that while Δ *glgC*, Δ *treS* and Δ Rv3032 single mutants, as well as Δ *glgC* Δ *treS* and Δ *glgC* Δ Rv3032 double mutants, were all viable, we could not inactivate Rv3032 in the Δ *treS* mutant. This suggested the joint essentiality of these two pathways. To corroborate this, we tested the sensitivity of the Mtb Δ Rv3032 mutant toward the TreS inhibitor validamycin A. Whereas the Mtb WT tolerated high concentrations of the inhibitor (10 mM), the Δ Rv3032 mutant was exceptionally sensitive to this compound, causing a 3-log killing over 7 d (Fig. 6a). Furthermore, overexpression of the putative target TreS conferred marked resistance of the Δ Rv3032 mutant to validamycin A (Fig. 6b). Together, these data unequivocally validate the joint essentiality (that is, the synthetic lethality) of *treS* and Rv3032.

DISCUSSION

The rapid emergence of XDR-TB strains highlights the urgent necessity of finding new classes of drugs to kill Mtb with new mechanisms of action. The paucity of new TB drugs discovered during the last few decades reflects our limited knowledge of essential metabolic processes in Mtb outside the repertoire of known targets such as transcription, translation or mycolic acid biosynthesis. In this study, a combination of genetic and biochemical studies has revealed that the M1P-dependent maltosyltransferase GlgE represents a potential new class of drug target, as it is part of a previously unrecognized α -glucan pathway that to our knowledge has never been targeted by antimicrobials. Studying the function of GlgE has revealed two new and distinct bactericidal mechanisms to induce death in Mtb. The first death mechanism is suicidal self-poisoning by accumulation of the phosphosugar M1P following GlgE inhibition. This process is likely driven by a self-amplifying feedback loop leading to trehalose release from glycogen via the GlgP-TreX-TreY-TreZ pathway, perhaps representing a misled stress protection response that further fuels the accumulation of M1P. The second (and independent) death mechanism is based on conditional essentiality of GlgE pathway products. Synthetic lethality of the GlgE and Rv3032 pathways indicates that they are involved in the production of related compounds that are reciprocally able to functionally compensate for metabolic or genetic perturbations in the other pathway. This explains why the GlgE pathway as a whole is fully dispensable for the viability and virulence of Mtb as long as the redundant Rv3032 pathway is functioning, but simultaneous inhibition of both pathways is lethal. Rv3032 is involved in the biosynthesis of methylglucosyl lipopolysaccharides (MGLPs). MGLPs are polymethylated α -glucan derivatives that are believed to play an essential regulatory role in fatty acid biosynthesis in Mtb²⁶. Therefore, GlgE pathway products are likely subject, at least partially, to further modifications, yielding so far unidentified derivatives structurally and/or functionally related to MGLPs (Fig. 3). Given that the two new bactericidal mechanisms in Mtb described above are separate and distinct, they will likely work in synergy. This means that, while monotherapy with GlgE inhibitors should be sufficient to kill Mtb as efficiently as treatment with the first-line drug isoniazid¹⁷, it will likely be possible to boost the potency of such GlgE inhibitors in a combination therapy with compounds inhibiting the synthetic lethal partner Rv3032. Furthermore, because every step of the GlgE pathway becomes essential when Rv3032 is inactive, combination therapy with Rv3032 inhibitors will also avoid resistance based on loss-of-function mutations in *treS* or *pep2* for evading M1P poisoning. The rapid emergence of such mutants *in vitro* and in mice indicates that preventing this type of suppressor mechanism could substantially increase the antitubercular potential of GlgE inhibitors.

This study has both therapeutic and general biological significance. We have established the existence of a previously unknown pathway, widespread among prokaryotes, for the conversion of trehalose to α -glucan. Possible connections between the metabolism of these compounds in bacteria have previously been proposed^{9,11,27}.

Our work now convincingly establishes the precise biochemical link through the GlgE pathway. This stems from our discovery that GlgE has a new maltosyltransferase activity of the Enzyme Commission number 2.4.1 hexosyltransferase type; GlgE thus will likely be assigned the systematic name (1→4)- α -D-glucan:phosphate α -D-maltosyltransferase. GlgE activity is consistent with a maltosyltransferase activity in protein extracts from *M. smegmatis* that was reported as the present study was in the final stages of review²⁸. Mtb GlgE is, according to the Carbohydrate Active Enzymes database (<http://www.cazy.org>; ref. 29) and based on its primary protein sequence, a member of the glycoside hydrolase subfamily GH13_3, to which no function has yet been ascribed³⁰. Although GlgE is a glycoside hydrolase GH family member and can catalyze transglucosylation reactions (that is, disproportionation), it is capable of glycosyltransfer reactions with the sugar phosphate donor M1P. This is a function more typically associated with members of the glycosyltransferase GT family, which use either nucleotide diphospho-sugar, nucleotide monophospho-sugar, polyprenyl phospho-sugar or phospho-sugar donors. For example, glycogen phosphorylase (systematic name (1→4)- α -D-glucan:phosphate α -D-glucosyltransferase; Enzyme Commission number 2.4.1.1) is a GT35 member. Sucrose phosphorylase (sucrose:phosphate α -D-glucosyltransferase; Enzyme Commission number 2.4.1.7), on the other hand, is a GH13_18 subfamily member, so GlgE is not the only GH13 family member to exhibit phosphorylase-type activity. Nevertheless, to our knowledge it is the first activity of this type described involving the transfer of disaccharide units. Furthermore, GlgE uniquely uses a sugar phosphate in a glycosyltransfer reaction for anabolic purposes. It therefore follows that although GlgE could be given the alternative informal name α -maltose 1-phosphate-forming α -(1,4)-glucan phosphorylase, this would reflect neither the physiologically relevant reaction that it catalyzes nor its intrinsic equilibrium. Our experimental evidence for both an α -retaining catalytic mechanism and a substituted-enzyme kinetic mechanism is consistent with the other GH13 family members that use a conserved aspartate side chain as a nucleophile to form a glycosyl-enzyme intermediate allowing an overall double displacement catalytic mechanism with net retention of stereochemistry³¹. Sequence alignments indicate that Asp418 is the likely nucleophilic residue in Mtb GlgE.

The physiological functions of the GlgE pathway remain elusive and could be multifaceted (Fig. 3). In addition to MGLP synthesis and in interaction with the Glc-GlgA and Rv3032 pathways, the GlgE pathway might alternatively participate in formation of the α -glucan capsule, an extracellular cell wall component potentially important for virulence and persistence of Mtb⁸. It could also be involved in the formation of intracellular glycogen, an α -glucan storage polymer from which trehalose can be remobilized via the GlgP-TreX-TreY-TreZ pathway to support trehalose homeostasis²⁴. Furthermore, because glycogen is a typical intracellular carbon storage compound in many organisms, the GlgE pathway might have a role in Mtb persistence within host microenvironments that exhibit restricted nutrient availability.

We have shown that essentiality of GlgE is based on direct or indirect toxicity of its substrate M1P. It has been proposed that the surprising essentiality of GlgB might be due to accumulation of poorly water-soluble linear α -1,4-glucan polymers that are hypothetically toxic³². However, the data presented here demonstrate that the toxicity of M1P, and not that of linear α -1,4-glucans, is the cause that underlies GlgB essentiality, which is explainable by GlgB's secondary effect on GlgE. In the absence of branching activity, GlgE produces linear α -1,4-glucans that not only have fewer nonreducing ends but also become insoluble once they reach a DP of ~20. Therefore, in the absence of GlgB, there will be fewer nonreducing ends available for GlgE to extend, retarding GlgE activity by acceptor substrate limitation that leads to a toxic buildup of M1P. Although

GlgB could be another potential drug target candidate, the existence of a human ortholog makes it less attractive than GlgE.

There is a widespread assertion that the biological function of TreS is to convert exclusively maltose to trehalose³³, despite the ready reversibility of this reaction. In at least those organisms that have a GlgE pathway, TreS now appears to catalyze the net reverse reaction *in vivo*. There is a report that *M. smegmatis* TreS enzyme also exhibits a minor catabolic amylase activity, allowing the direct conversion of glycogen to maltose⁹, although this activity is two orders of magnitude lower than the normal TreS reaction. In addition, the amylase activity does not appear to be physiologically significant because the same authors reported that glycogen accumulated in the wild-type organism, but not in a *treS* mutant, when grown specifically in the presence of trehalose, supporting a dominant anabolic role for TreS.

Why is M1P toxic? M1P accumulation as a result of GlgE inactivation appears to elicit pleiotropic stresses in Mtb, including inhibition of respiration, induction of the stringent response and DNA damage. Because Mtb can tolerate respiration inhibitors relatively well under aerobic conditions^{18,19} and also maintains viability under conditions such as starvation that trigger the stringent response, DNA damage is probably the most critical factor leading to death. DNA damage might be an indirect result of disturbed respiration, potentially leading to the generation of reactive oxygen species. In *Escherichia coli*, upregulation of NADH dehydrogenase I was found to be a common key response to all tested bactericidal drugs that all lead to hydroxyl radical formation and subsequent induction of the DNA damage-triggered SOS response³⁴. Notably, upregulation of components of NADH dehydrogenase I (*nuoB*, *nuoD*, *nuoE* and *nuoF*) was also observed in M1P-stressed Mtb cultures. This suggests that M1P-induced lethality might share certain aspects of the common mechanism of cellular death caused by bactericidal antibiotics in *E. coli*³⁴. However, although the observed stress phenotypes are unequivocally associated with M1P accumulation, it cannot be excluded that M1P might not be directly toxic to the cells but could rather lead indirectly to toxicity by complex mechanisms—for example, through some unidentified degradation or shunt products. Clearly, more work is needed to unravel the exact molecular toxicity mechanisms associated with M1P accumulation that eventually lead to DNA damage and death.

In summary, the unique combination of gene essentiality within a synthetic lethal pathway, revealing potential mechanisms not only to boost the potency of inhibitors but also to suppress resistance mutations, distinguishes GlgE from all Mtb drug targets described so far. Self-poisoning by a phosphosugar provoking pleiotropic stresses through direct or indirect toxicity also implies a new mechanism to induce death in Mtb that is different from those used by current TB drugs and reveals α -glucan synthesis as a potential target for antimicrobials. Thus, there is reason to believe that GlgE inhibitors, enhanced by Rv3032 inhibitors, could be developed to treat XDR-TB. However, it has to be noted that such a specifically enhancing combination therapy would be a new path in the anti-infective drug discovery field, which so far only focuses on monotherapy. Nonetheless, this study exemplifies the great potential for the discovery of new TB drug targets hidden within synthetic lethal pathways.

METHODS

Generation of gene deletion mutants. Mutants of *M. smegmatis* mc²155 and Mtb H37Rv were generated by allelic exchange using specialized transduction³⁵ as described in detail in the **Supplementary Methods**.

Carbohydrate TLC analysis. Carbohydrates were extracted from equal amounts of cells with hot water (95 °C for 4 h) and analyzed by TLC on silica gel 60 (EMD Chemicals) using the solvent system 1-propanol:ethyl acetate:water (6:1:3, v/v/v). For separation of trehalose and maltose, the solvent system *n*-butanol:pyridine:water (7:3:1, v/v/v) was used. ¹⁴C- α -D-trehalose (specific activity 300 mCi mmol⁻¹; American Radiolabeled Chemicals) was used in some

experiments at a concentration of 0.1 $\mu\text{Ci ml}^{-1}$. Substances were visualized by spraying TLC plates with 10% (v/v) sulfuric acid in ethanol followed by charring at 180 °C for 10 min, or by autoradiography where applicable.

Purification and assay of Mtb GlgE. The Mtb *glgE* gene was synthesized with optimized codon usage for expression in *E. coli* (Genscript Corporation), heterologously expressed with an N-terminal 6 \times histidine tag, and purified using nickel-affinity and gel filtration chromatographies as described in the **Supplementary Methods**. GlgE activity was monitored quantitatively by the release of inorganic phosphate using malachite green colorimetric detection³⁶. Initial rates ($v_0/[E]$) were measured by quenching 3 μl reaction aliquots in 97 μl of 1 M HCl at time points from 0.5 to 8 min. The quenched reactions were incubated with 700 μl of malachite green assay solution for 20 min at 21 °C, and the optical density at 630 nm (OD_{630}) was measured on a Perkin Elmer Lambda 18 spectrophotometer. The concentration of free inorganic phosphate was estimated from a standard curve. Reaction rates were linear over at least the first 4 min. Unless otherwise stated, the enzyme assay was done in 100 mM Bis-Tris propane (pH 7.0) containing 50 mM NaCl at 37 °C. Acceptor preference was examined in triplicate using 40 mM maltooligosaccharide, 1 mM α -MIP (its synthesis, together with that of the β -anomer, will be reported elsewhere) and 37.5 nM Mtb GlgE.

MALDI mass spectrometry. For qualitative analyses of maltooligosaccharide elongation, GlgE assays were performed with typically 12.5 mM α -MIP and 1.5 μM Mtb GlgE. Aliquots (1 μl) of reaction mixtures were diluted 50-fold in H_2O , mixed 1:1 with saturated aqueous 2,5-dihydroxybenzoic acid, loaded (1 μl) onto a gold target plate, and dried under vacuum. Analysis was carried out on a PBS-II mass spectrometer using ProteinChip 3.0 software (Ciphergen Biosystems Inc.).

NMR linkage analysis. A reaction (25 μl) containing 20 mM maltotetraose, 20 mM α -MIP, and 1.2 μM Mtb GlgE was allowed to reach completion according to the phosphate release assay. The reaction was heated to 99 °C for 15 min, cooled and diluted to 500 μl with D_2O . A control reaction without enzyme was also prepared. One-dimensional ^1H spectra were recorded on an AVANCE 600 with TCI cryoprobe at 600 MHz and 300 K and analyzed with Topspin 2.1 software (Bruker Biospin Ltd.). Spectra were acquired with presaturation to suppress the water peak.

DNA microarrays and qRT-PCR. Triplicate 10 ml cultures of the conditional lethal Mtb mutant strain $\Delta treS \Delta glgE$ (pMV361::*treS*) and of the vector control strain were grown to log phase in the presence of 5 mM validamycin A to suppress MIP formation. Subsequently, cells were washed to remove the inhibitor. After 48 h of depletion of validamycin A, cells were harvested, resuspended in 1 ml Qiagen RNA Protect reagent (Qiagen) and incubated 4 h at room temperature (21 °C). RNA was isolated by bead beating in a Fast-Prep apparatus (MP Biomedicals) and using the Qiagen RNeasy kit according to protocol. Contaminating DNA was removed with the Ambion TURBO DNA-free kit (Applied Biosystems). DNA microarrays were obtained through the US National Institute of Allergy and Infectious Diseases' Pathogen Functional Genomics Resource Center (PFGRC, funded by the Division of Microbiology and Infectious Diseases, National Institute of Allergy and Infectious Diseases, National Institutes of Health, Department of Health and Human Services, and operated by the J. Craig Venter Institute). cDNA probes were prepared as per PFGRC protocol SOP#M007 (<http://pfgrc.jcvi.org/index.php/microarray/protocols.html>). Cy3- and Cy5-labeled cDNA probes were hybridized according to PFGRC protocol SOP#M008 (70-mer oligo DNA microarrays representing the complete *M. tuberculosis* genome (JCVI PFGRC *M. tuberculosis* v. 4). One of the three biological replicates was dye-flipped. Slides were scanned on a GenePix 4000A scanner (Molecular Devices). Images were processed with the TM4 software suite³⁷. TIGR Spotfinder was used to grid and quantitate spots. TIGR MIDAS was used for Lowess normalization, s.d. regularization, and in-slide replicate analysis with all quality control flags on and one bad channel tolerance policy set to 'generous'. Results were analyzed in MeV with significance analysis of microarrays (SAM) considered significant at $q < 0.05$. Microarray data have been deposited in the US National Center for Biotechnology Information Gene Expression Omnibus (GEO series accession number GSE18575).

For qRT-PCR, the DNA-free RNA samples used for the microarray experiments were reverse transcribed with the SuperScript III First-Strand Synthesis System (Invitrogen). For the real-time reaction, each primer (250 nM) and 7.5 μl of template reaction (1:20 dilution) in 25 μl volume with Power SYBR Green PCR master mix (Applied Biosystems) was used. Triplicate samples were run on an ABI 7900 HT quantitative thermocycler. Threshold cycles were normalized to those for 16S rRNA and to total RNA. Primer sequences used for qRT-PCR are listed in **Supplementary Table 1**.

Animal infections. BALB/c mice (4- to 6-week-old females; US National Cancer Institute) were infected intravenously through the lateral tail vein at the indicated doses with exponentially growing Mtb strains suspended in 200 μl phosphate-buffered saline containing 0.05% (v/v) Tween 80. At different time points, three mice per group were killed, and bacterial burden was determined by plating serial dilutions of lung and spleen homogenates onto Middlebrook 7H10 agar plates supplemented with 10% (v/v) OADC enrichment (Becton

Dickinson Microbiology Systems) and 0.5% (v/v) glycerol. Plates contained 5 mM validamycin A for the conditional lethal Mtb mutant strain $\Delta treS \Delta glgE$ (pMV361::*treS*). Mouse protocols were approved by the Animal Care and Use Committee of the Albert Einstein College of Medicine.

Other methods. See the **Supplementary Methods** for more detailed methods, including strains (**Supplementary Table 2**), growth conditions, oligonucleotide sequences (**Supplementary Tables 1 and 3**) and further chemical analyses.

Accession codes. Gene Expression Omnibus: Microarray data have been deposited in the US National Center for Biotechnology Information Gene Expression Omnibus (GEO series accession number GSE18575).

Received 20 October 2009; accepted 16 February 2010; published online 21 March 2010

References

- Dye, C. Global epidemiology of tuberculosis. *Lancet* **367**, 938–940 (2006).
- Sassetti, C.M., Boyd, D.H. & Rubin, E.J. Genes required for mycobacterial growth defined by high density mutagenesis. *Mol. Microbiol.* **48**, 77–84 (2003).
- Sassetti, C.M. & Rubin, E.J. Genetic requirements for mycobacterial survival during infection. *Proc. Natl. Acad. Sci. USA* **100**, 12989–12994 (2003).
- Tong, A.H. *et al.* Global mapping of the yeast genetic interaction network. *Science* **303**, 808–813 (2004).
- Boone, C., Bussey, H. & Andrews, B.J. Exploring genetic interactions and networks with yeast. *Nat. Rev. Genet.* **8**, 437–449 (2007).
- Belanger, A.E. & Hatfull, G.F. Exponential-phase glycogen recycling is essential for growth of *Mycobacterium smegmatis*. *J. Bacteriol.* **181**, 6670–6678 (1999).
- Garg, S.K., Alam, M.S., Kishan, K.V. & Agrawal, P. Expression and characterization of alpha-(1,4)-glucan branching enzyme Rv1326c of *Mycobacterium tuberculosis* H37Rv. *Protein Expr. Purif.* **51**, 198–208 (2007).
- Sambou, T. *et al.* Capsular glucan and intracellular glycogen of *Mycobacterium tuberculosis*: biosynthesis and impact on the persistence in mice. *Mol. Microbiol.* **70**, 762–774 (2008).
- Pan, Y.T. *et al.* Trehalose synthase converts glycogen to trehalose. *FEBS J.* **275**, 3408–3420 (2008).
- Pan, Y.T. *et al.* Trehalose synthase of *Mycobacterium smegmatis*: purification, cloning, expression, and properties of the enzyme. *Eur. J. Biochem.* **271**, 4259–4269 (2004).
- Jarling, M., Cauvet, T., Grundmeier, M., Kuhnert, K. & Pape, H. Isolation of *mak1* from *Actinoplanes missouriensis* and evidence that *Pep2* from *Streptomyces coelicolor* is a maltokinase. *J. Basic Microbiol.* **44**, 360–373 (2004).
- Usui, T. *et al.* Proton magnetic resonance spectra of D-glucosyloligosaccharides and D-glucans. *Carbohydr. Res.* **33**, 105–116 (1974).
- Bosch, A.M. Classical galactosaemia revisited. *J. Inher. Metab. Dis.* **29**, 516–525 (2006).
- Slepek, T., Tang, M., Addo, F. & Lai, K. Intracellular galactose-1-phosphate accumulation leads to environmental stress response in yeast model. *Mol. Genet. Metab.* **86**, 360–371 (2005).
- Yarmolinsky, M.B., Wiesmeyer, H., Kalckar, H.M. & Jordan, E. Hereditary defects in galactose metabolism in *Escherichia coli* mutants, II. Galactose-induced sensitivity. *Proc. Natl. Acad. Sci. USA* **45**, 1786–1791 (1959).
- Streeter, J.G. & Gomez, M.L. Three enzymes for trehalose synthesis in *Bradyrhizobium* cultured bacteria and in bacteroids from soybean nodules. *Appl. Environ. Microbiol.* **72**, 4250–4255 (2006).
- Karakousis, P.C., Williams, E.P. & Bishai, W.R. Altered expression of isoniazid-regulated genes in drug-treated dormant *Mycobacterium tuberculosis*. *J. Antimicrob. Chemother.* **61**, 323–331 (2008).
- Boshoff, H.I. *et al.* The transcriptional responses of *Mycobacterium tuberculosis* to inhibitors of metabolism: novel insights into drug mechanisms of action. *J. Biol. Chem.* **279**, 40174–40184 (2004).
- Manjunatha, U., Boshoff, H.I. & Barry, C.E. The mechanism of action of PA-824: novel insights from transcriptional profiling. *Commun. Integr. Biol.* **2**, 215–218 (2009).
- Kumar, A. *et al.* Heme oxygenase-1-derived carbon monoxide induces the *Mycobacterium tuberculosis* dormancy regulon. *J. Biol. Chem.* **283**, 18032–18039 (2008).
- Voskuil, M.I. *et al.* Inhibition of respiration by nitric oxide induces a *Mycobacterium tuberculosis* dormancy program. *J. Exp. Med.* **198**, 705–713 (2003).
- Dahl, J.L. *et al.* The role of Rel_{Mtb}-mediated adaptation to stationary phase in long-term persistence of *Mycobacterium tuberculosis* in mice. *Proc. Natl. Acad. Sci. USA* **100**, 10026–10031 (2003).
- Boshoff, H.I., Reed, M.B., Barry, C.E. III & Mizrahi, V. DnaE2 polymerase contributes to in vivo survival and the emergence of drug resistance in *Mycobacterium tuberculosis*. *Cell* **113**, 183–193 (2003).
- Murphy, H.N. *et al.* The OtsAB pathway is essential for trehalose biosynthesis in *Mycobacterium tuberculosis*. *J. Biol. Chem.* **280**, 14524–14529 (2005).

25. Arguelles, J.C. Physiological roles of trehalose in bacteria and yeasts: a comparative analysis. *Arch. Microbiol.* **174**, 217–224 (2000).
26. Jackson, M. & Brennan, P.J. Polymethylated polysaccharides from *Mycobacterium* species revisited. *J. Biol. Chem.* **284**, 1949–1953 (2009).
27. Schneider, D., Bruton, C.J. & Chater, K.F. Duplicated gene clusters suggest an interplay of glycogen and trehalose metabolism during sequential stages of aerial mycelium development in *Streptomyces coelicolor* A3(2). *Mol. Gen. Genet.* **263**, 543–553 (2000).
28. Elbein, A.D., Pastuszak, I., Tackett, A.J., Wilson, T. & Pan, Y.T. The last step in the conversion of trehalose to glycogen: a mycobacterial enzyme that transfers maltose from maltose-1-phosphate to glycogen. *J. Biol. Chem.* published online, doi:10.1074/jbc.M109.033944 (29 January 2010).
29. Cantarel, B.L. *et al.* The Carbohydrate-Active EnZymes database (CAZy): an expert resource for glycogenomics. *Nucleic Acids Res.* **37**, D233–D238 (2009).
30. Stam, M.R., Danchin, E.G.J., Rancurel, C., Coutinho, P.M. & Henrissat, B. Dividing the large glycoside hydrolase family 13 into subfamilies: towards improved functional annotations of α -amylase-related proteins. *Protein Eng. Des. Sel.* **19**, 555–562 (2006).
31. McCarter, J.D. & Withers, S.G. Unequivocal identification of Asp-214 as the catalytic nucleophile of *Saccharomyces cerevisiae* alpha-glucosidase using 5-fluoro glycosyl fluorides. *J. Biol. Chem.* **271**, 6889–6894 (1996).
32. Kaur, D., Guerin, M.E., Skovierova, H., Brennan, P.J. & Jackson, M. Chapter 2 Biogenesis of the cell wall and other glycoconjugates of *Mycobacterium tuberculosis*. *Adv. Appl. Microbiol.* **69**, 23–78 (2009).
33. Elbein, A.D., Pan, Y.T., Pastuszak, I. & Carroll, D. New insights on trehalose: a multifunctional molecule. *Glycobiology* **13**, 17R–27R (2003).
34. Kohanski, M.A., Dwyer, D.J., Hayete, B., Lawrence, C.A. & Collins, J.J. A common mechanism of cellular death induced by bactericidal antibiotics. *Cell* **130**, 797–810 (2007).
35. Bardarov, S. *et al.* Specialized transduction: an efficient method for generating marked and unmarked targeted gene disruptions in *Mycobacterium tuberculosis*, *M. bovis* BCG and *M. smegmatis*. *Microbiology* **148**, 3007–3017 (2002).
36. Lanzetta, P.A., Alvarez, L.J., Remack, P.S. & Candia, O.A. An improved assay for nanomole amounts of inorganic phosphate. *Anal. Biochem.* **100**, 95–97 (1979).
37. Saeed, A.I. *et al.* TM4: a free, open-source system for microarray data management and analysis. *Biotechniques* **34**, 374–378 (2003).

Acknowledgments

We thank G. Hatfull for promoting a collaboration between the Bornemann and Jacobs labs. This work was supported by US National Institutes of Health grants AI26170 (to W.R.J.) and AIO-68135 (Structural Biology of TB Drug Targets), the Albert Einstein College of Medicine Center for AIDS Research grant AIO-51519 and the UK Biotechnology and Biological Sciences Research Council through an Institute Strategic Programme Grant to the John Innes Centre. We thank C. Bruton and K. Chater for access to unpublished data and insightful discussions, D. Hopwood for advice on the manuscript and S. Fairhurst and L. Hill for recording NMR and mass spectra at the John Innes Centre. G.B. acknowledges support in the form of a Personal Research Chair from J. Bardrick (Royal Society Wolfson Research Merit Award, as a former Lister Institute Jenner Research Fellow). G.B. also acknowledges support from The Medical Research Council and the Wellcome Trust (081569/2/06/2). We thank P. Illarionov for discussion of NMR results and the staff in technical services of the University of Birmingham (especially N. Spencer, G. Burns and P. Ashton) for help in the NMR, GC and ES-MS experiments. This paper is dedicated to the late Chris Lamb.

Author contributions

R.K., S.B. and W.R.J. coordinated the study. R.K., K.S., U.V., B.W. and K.E.B. performed experiments. R.K., K.S., U.V., B.W., G.B. and S.B. analyzed data. Z.L. and J.C.S. provided reagents. R.K., S.B. and W.R.J. wrote the paper and K.S., U.V., B.W. and G.B. edited the paper.

Competing financial interests

The authors declare no competing financial interests.

Additional information

Supplementary information is available online at <http://www.nature.com/naturechemicalbiology/>. Reprints and permissions information is available online at <http://npg.nature.com/reprintsandpermissions/>. Correspondence and requests for materials should be addressed to W.R.J.